

# 31

---

## Ising Models

An Ising model is an array of spins (e.g., atoms that can take states  $\pm 1$ ) that are magnetically coupled to each other. If one spin is, say, in the  $+1$  state then it is energetically favourable for its immediate neighbours to be in the same state, in the case of a ferromagnetic model, and in the opposite state, in the case of an antiferromagnet. In this chapter we discuss two computational techniques for studying Ising models.

Let the state  $\mathbf{x}$  of an Ising model with  $N$  spins be a vector in which each component  $x_n$  takes values  $-1$  or  $+1$ . If two spins  $m$  and  $n$  are neighbours we write  $(m, n) \in \mathcal{N}$ . The coupling between neighbouring spins is  $J$ . We define  $J_{mn} = J$  if  $m$  and  $n$  are neighbours and  $J_{mn} = 0$  otherwise. The energy of a state  $\mathbf{x}$  is

$$E(\mathbf{x}; J, H) = - \left[ \frac{1}{2} \sum_{m,n} J_{mn} x_m x_n + \sum_n H x_n \right], \quad (31.1)$$

where  $H$  is the applied field. If  $J > 0$  then the model is ferromagnetic, and if  $J < 0$  it is antiferromagnetic. We've included the factor of  $1/2$  because each pair is counted twice in the first sum, once as  $(m, n)$  and once as  $(n, m)$ . At equilibrium at temperature  $T$ , the probability that the state is  $\mathbf{x}$  is

$$P(\mathbf{x} | \beta, J, H) = \frac{1}{Z(\beta, J, H)} \exp[-\beta E(\mathbf{x}; J, H)], \quad (31.2)$$

where  $\beta = 1/k_B T$ ,  $k_B$  is Boltzmann's constant, and

$$Z(\beta, J, H) \equiv \sum_{\mathbf{x}} \exp[-\beta E(\mathbf{x}; J, H)]. \quad (31.3)$$

### Relevance of Ising models

Ising models are relevant for three reasons.

Ising models are important first as models of magnetic systems that have a phase transition. The theory of universality in statistical physics shows that all systems with the same dimension (here, two), and the same symmetries, have equivalent critical properties, i.e., the scaling laws shown by their phase transitions are identical. So by studying Ising models we can find out not only about magnetic phase transitions but also about phase transitions in many other systems.

Second, if we generalize the energy function to

$$E(\mathbf{x}; \mathbf{J}, \mathbf{h}) = - \left[ \frac{1}{2} \sum_{m,n} J_{mn} x_m x_n + \sum_n h_n x_n \right], \quad (31.4)$$

where the couplings  $J_{mn}$  and applied fields  $h_n$  are not constant, we obtain a family of models known as 'spin glasses' to physicists, and as 'Hopfield

networks' or 'Boltzmann machines' to the neural network community. In some of these models, all spins are declared to be neighbours of each other, in which case physicists call the system an 'infinite-range' spin glass, and networkers call it a 'fully connected' network.

Third, the Ising model is also useful as a statistical model in its own right.

In this chapter we will study Ising models using two different computational techniques.

### *Some remarkable relationships in statistical physics*

We would like to get as much information as possible out of our computations. Consider for example the heat capacity of a system, which is defined to be

$$C \equiv \frac{\partial}{\partial T} \bar{E}, \quad (31.5)$$

where

$$\bar{E} = \frac{1}{Z} \sum_{\mathbf{x}} \exp(-\beta E(\mathbf{x})) E(\mathbf{x}). \quad (31.6)$$

To work out the heat capacity of a system, we might naively guess that we have to increase the temperature and measure the energy change. Heat capacity, however, is intimately related to energy *fluctuations* at constant temperature. Let's start from the partition function,

$$Z = \sum_{\mathbf{x}} \exp(-\beta E(\mathbf{x})). \quad (31.7)$$

The mean energy is obtained by differentiation with respect to  $\beta$ :

$$\frac{\partial \ln Z}{\partial \beta} = \frac{1}{Z} \sum_{\mathbf{x}} -E(\mathbf{x}) \exp(-\beta E(\mathbf{x})) = -\bar{E}. \quad (31.8)$$

A further differentiation spits out the variance of the energy:

$$\frac{\partial^2 \ln Z}{\partial \beta^2} = \frac{1}{Z} \sum_{\mathbf{x}} E(\mathbf{x})^2 \exp(-\beta E(\mathbf{x})) - \bar{E}^2 = \langle E^2 \rangle - \bar{E}^2 = \text{var}(E). \quad (31.9)$$

But the heat capacity is also the derivative of  $\bar{E}$  with respect to temperature:

$$\frac{\partial \bar{E}}{\partial T} = -\frac{\partial}{\partial T} \frac{\partial \ln Z}{\partial \beta} = -\frac{\partial^2 \ln Z}{\partial \beta^2} \frac{\partial \beta}{\partial T} = -\text{var}(E)(-1/k_B T^2). \quad (31.10)$$

So for any system at temperature  $T$ ,

$$C = \frac{\text{var}(E)}{k_B T^2} = k_B \beta^2 \text{var}(E). \quad (31.11)$$

Thus if we can observe the variance of the energy of a system at equilibrium, we can estimate its heat capacity.

I find this an almost paradoxical relationship. Consider a system with a finite set of states, and imagine heating it up. At high temperature, all states will be equiprobable, so the mean energy will be essentially constant and the heat capacity will be essentially zero. But on the other hand, with all states being equiprobable, there will certainly be fluctuations in energy. So how can the heat capacity be related to the fluctuations? The answer is in the words 'essentially zero' above. The heat capacity is not quite zero at high temperature, it just tends to zero. And it tends to zero as  $\frac{\text{var}(E)}{k_B T^2}$ , with

the quantity  $\text{var}(E)$  tending to a constant at high temperatures. This  $1/T^2$  behaviour of the heat capacity of finite systems at high temperatures is thus very general.

The  $1/T^2$  factor can be viewed as an accident of history. If only temperature scales had been defined using  $\beta = \frac{1}{k_B T}$ , then the definition of heat capacity would be

$$C^{(\beta)} \equiv \frac{\partial \bar{E}}{\partial \beta} = \text{var}(E), \quad (31.12)$$

and heat capacity and fluctuations would be identical quantities.

▷ **Exercise 31.1.**<sup>[2]</sup> [We will call the entropy of a physical system  $S$  rather than  $H$ , while we are in a statistical physics chapter; we set  $k_B = 1$ .]

The entropy of a system whose states are  $\mathbf{x}$ , at temperature  $T = 1/\beta$ , is

$$S = -\sum p(\mathbf{x}) [\ln 1/p(\mathbf{x})] \quad (31.13)$$

where

$$p(\mathbf{x}) = \frac{1}{Z(\beta)} \exp[-\beta E(\mathbf{x})]. \quad (31.14)$$

(a) Show that

$$S = \ln Z(\beta) + \beta \bar{E}(\beta) \quad (31.15)$$

where  $\bar{E}(\beta)$  is the mean energy of the system.

(b) Show that

$$S = -\frac{\partial F}{\partial T}, \quad (31.16)$$

where the free energy  $F = -kT \ln Z$  and  $kT = 1/\beta$ .

### ► 31.1 Ising models – Monte Carlo simulation

In this section we study two-dimensional planar Ising models using a simple Gibbs-sampling method. Starting from some initial state, a spin  $n$  is selected at random, and the probability that it should be  $+1$  given the state of the other spins and the temperature is computed,

$$P(+1 | b_n) = \frac{1}{1 + \exp(-2\beta b_n)}, \quad (31.17)$$

where  $\beta = 1/k_B T$  and  $b_n$  is the local field

$$b_n = \sum_{m: (m,n) \in \mathcal{N}} Jx_m + H. \quad (31.18)$$

[The factor of 2 appears in equation (31.17) because the two spin states are  $\{+1, -1\}$  rather than  $\{+1, 0\}$ .] Spin  $n$  is set to  $+1$  with that probability, and otherwise to  $-1$ ; then the next spin to update is selected at random. After sufficiently many iterations, this procedure converges to the equilibrium distribution (31.2). An alternative to the Gibbs sampling formula (31.17) is the Metropolis algorithm, in which we consider the change in energy that results from flipping the chosen spin from its current state  $x_n$ ,

$$\Delta E = 2x_n b_n, \quad (31.19)$$

and adopt this change in configuration with probability

$$P(\text{accept}; \Delta E, \beta) = \begin{cases} 1 & \Delta E \leq 0 \\ \exp(-\beta \Delta E) & \Delta E > 0. \end{cases} \quad (31.20)$$

### 31.1: Ising models – Monte Carlo simulation

403

This procedure has roughly double the probability of accepting energetically unfavourable moves, so may be a more efficient sampler – but at very low temperatures the relative merits of Gibbs sampling and the Metropolis algorithm may be subtle.

#### Rectangular geometry

I first simulated an Ising model with the rectangular geometry shown in figure 31.1, and with periodic boundary conditions. A line between two spins indicates that they are neighbours. I set the external field  $H = 0$  and considered the two cases  $J = \pm 1$ , which are a ferromagnet and antiferromagnet respectively.

I started at a large temperature ( $T = 33, \beta = 0.03$ ) and changed the temperature every  $I$  iterations, first decreasing it gradually to  $T = 0.1, \beta = 10$ , then increasing it gradually back to a large temperature again. This procedure gives a crude check on whether ‘equilibrium has been reached’ at each temperature; if not, we’d expect to see some hysteresis in the graphs we plot. It also gives an idea of the reproducibility of the results, if we assume that the two runs, with decreasing and increasing temperature, are effectively independent of each other.

At each temperature I recorded the mean energy per spin and the standard deviation of the energy, and the mean square value of the magnetization  $m$ ,

$$m = \frac{1}{N} \sum_n x_n. \quad (31.21)$$

One tricky decision that has to be made is how soon to start taking these measurements after a new temperature has been established; it is difficult to detect ‘equilibrium’ – or even to give a clear definition of a system’s being ‘at equilibrium’! [But in Chapter 32 we will see a solution to this problem.] My crude strategy was to let the number of iterations at each temperature,  $I$ , be a few hundred times the number of spins  $N$ , and to discard the first  $1/3$  of those iterations. With  $N = 100$ , I found I needed more than 100 000 iterations to reach equilibrium at any given temperature.

#### Results for small $N$ with $J = 1$ .

I simulated an  $l \times l$  grid for  $l = 4, 5, \dots, 10, 40, 64$ . Let’s have a quick think about what results we expect. At low temperatures the system is expected to be in a ground state. The rectangular Ising model with  $J = 1$  has two ground states, the all  $+1$  state and the all  $-1$  state. The energy per spin of either ground state is  $-2$ . At high temperatures, the spins are independent, all states are equally probable, and the energy is expected to fluctuate around a mean of 0 with a standard deviation proportional to  $1/\sqrt{N}$ .

Let’s look at some results. In all figures temperature  $T$  is shown with  $k_B = 1$ . The basic picture emerges with as few as 16 spins (figure 31.3, top): the energy rises monotonically. As we increase the number of spins to 100 (figure 31.3, bottom) some new details emerge. First, as expected, the fluctuations at large temperature decrease as  $1/\sqrt{N}$ . Second, the fluctuations at intermediate temperature become relatively *bigger*. This is the signature of a ‘collective phenomenon’, in this case, a phase transition. Only systems with infinite  $N$  show true phase transitions, but with  $N = 100$  we are getting a hint of the critical fluctuations. Figure 31.5 shows details of the graphs for  $N = 100$  and  $N = 4096$ . Figure 31.2 shows a sequence of typical states from the simulation of  $N = 4096$  spins at a sequence of decreasing temperatures.

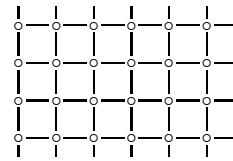


Figure 31.1. Rectangular Ising model.

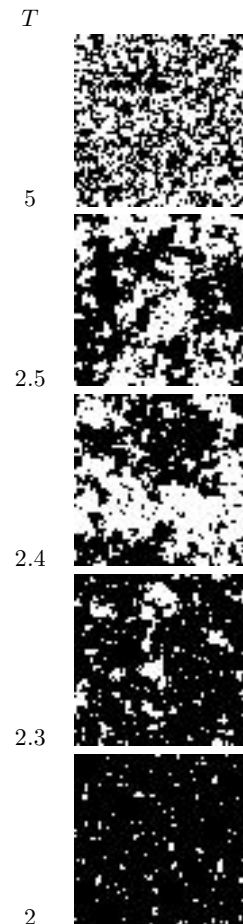


Figure 31.2. Sample states of rectangular Ising models with  $J = 1$  at a sequence of temperatures  $T$ .

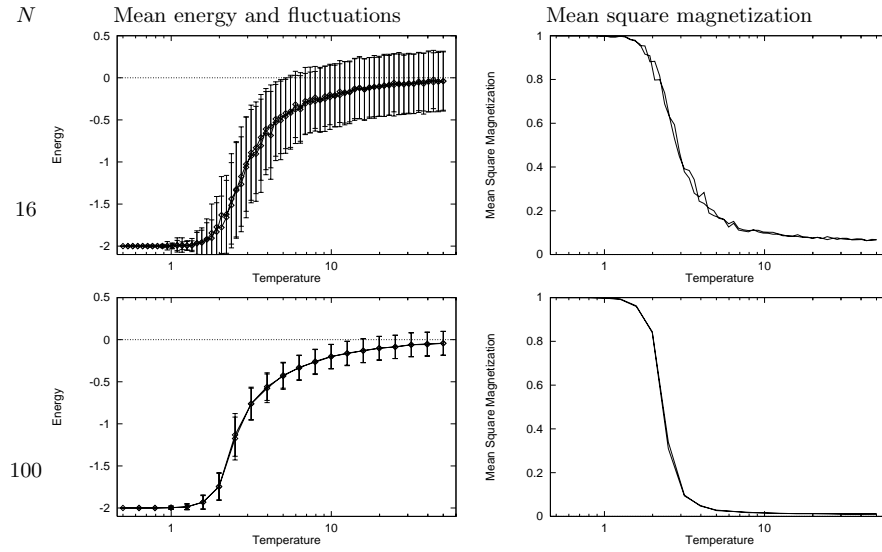


Figure 31.3. Monte Carlo simulations of rectangular Ising models with  $J = 1$ . Mean energy and fluctuations in energy as a function of temperature (left). Mean square magnetization as a function of temperature (right). In the top row,  $N = 16$ , and the bottom,  $N = 100$ . For even larger  $N$ , see later figures.

### Contrast with Schottky anomaly

A peak in the heat capacity, as a function of temperature, occurs in any system that has a finite number of energy levels; a peak is not in itself evidence of a phase transition. Such peaks were viewed as anomalies in classical thermodynamics, since ‘normal’ systems with infinite numbers of energy levels (such as a particle in a box) have heat capacities that are either constant or increasing functions of temperature. In contrast, systems with a finite number of levels produced small blips in the heat capacity graph (figure 31.4).

Let us refresh our memory of the simplest such system, a two-level system with states  $x = 0$  (energy 0) and  $x = 1$  (energy  $\epsilon$ ). The mean energy is

$$E(\beta) = \epsilon \frac{\exp(-\beta\epsilon)}{1 + \exp(-\beta\epsilon)} = \epsilon \frac{1}{1 + \exp(\beta\epsilon)} \quad (31.22)$$

and the derivative with respect to  $\beta$  is

$$dE/d\beta = -\epsilon^2 \frac{\exp(\beta\epsilon)}{[1 + \exp(\beta\epsilon)]^2}. \quad (31.23)$$

So the heat capacity is

$$C = dE/dT = -\frac{dE}{d\beta} \frac{1}{k_B T^2} = \frac{\epsilon^2}{k_B T^2} \frac{\exp(\beta\epsilon)}{[1 + \exp(\beta\epsilon)]^2} \quad (31.24)$$

and the fluctuations in energy are given by  $\text{var}(E) = C k_B T^2 = -dE/d\beta$ , which was evaluated in (31.23). The heat capacity and fluctuations are plotted in figure 31.6. The take-home message at this point is that whilst Schottky anomalies do have a peak in the heat capacity, there is *no* peak in their *fluctuations*; the variance of the energy simply increases monotonically with temperature to a value proportional to the number of independent spins. Thus it is a peak in the *fluctuations* that is interesting, rather than a peak in the heat capacity. The Ising model has such a peak in its fluctuations, as can be seen in the second row of figure 31.5.

### Rectangular Ising model with $J = -1$

What do we expect to happen in the case  $J = -1$ ? The ground states of an infinite system are the two checkerboard patterns (figure 31.7), and they have

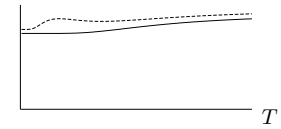


Figure 31.4. Schematic diagram to explain the meaning of a Schottky anomaly. The curve shows the heat capacity of two gases as a function of temperature. The lower curve shows a normal gas whose heat capacity is an increasing function of temperature. The upper curve has a small peak in the heat capacity, which is known as a Schottky anomaly (at least in Cambridge). The peak is produced by the gas having magnetic degrees of freedom with a finite number of accessible states.

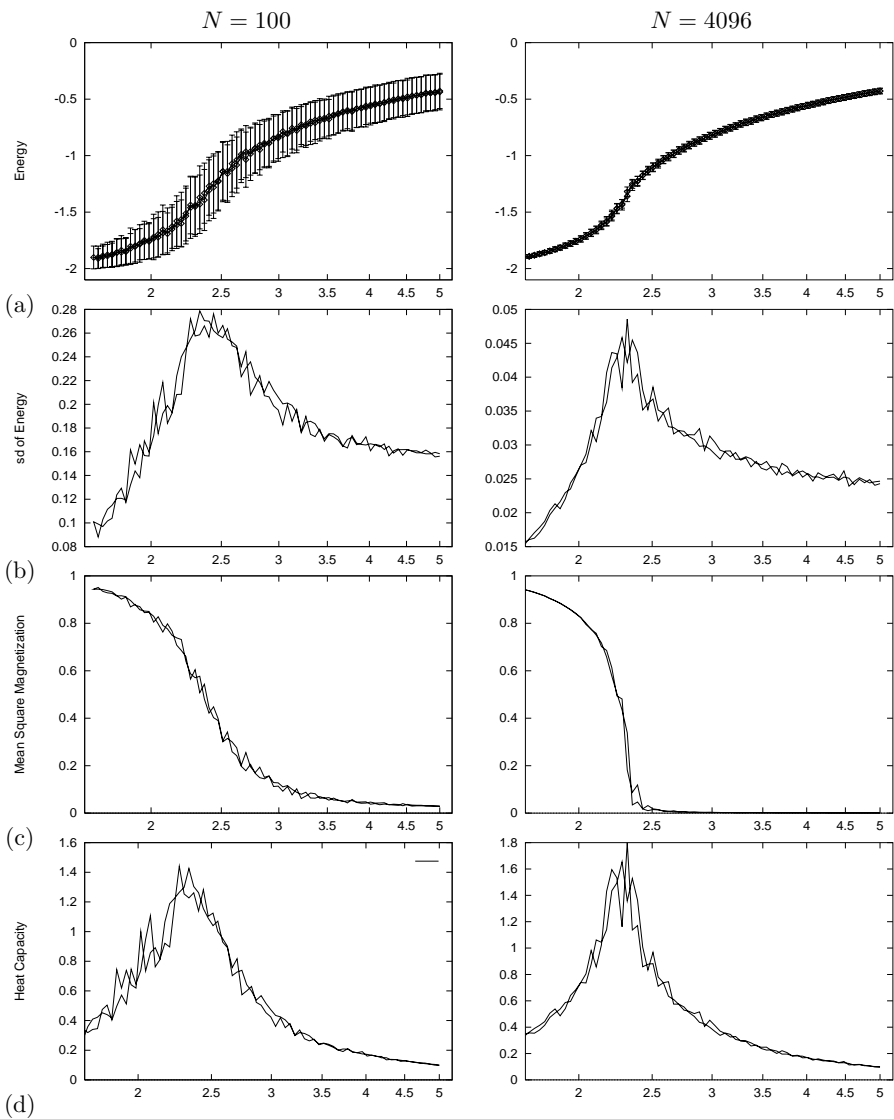


Figure 31.5. Detail of Monte Carlo simulations of rectangular Ising models with  $J = 1$ . (a) Mean energy and fluctuations in energy as a function of temperature. (b) Fluctuations in energy (standard deviation). (c) Mean square magnetization. (d) Heat capacity.

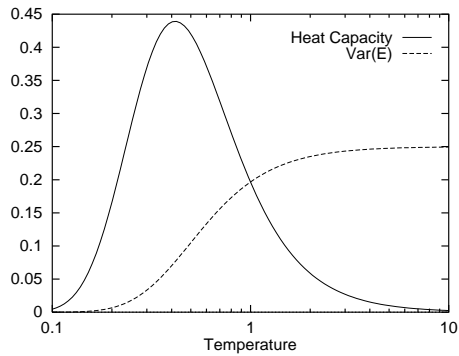
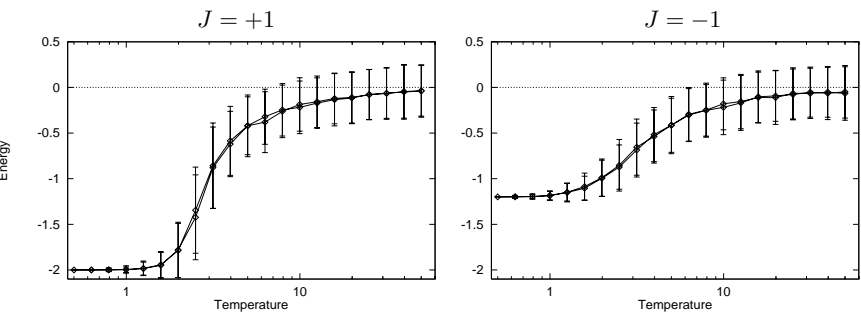


Figure 31.6. Schottky anomaly – Heat capacity and fluctuations in energy as a function of temperature for a two-level system with separation  $\epsilon = 1$  and  $k_B = 1$ .

energy per spin  $-2$ , like the ground states of the  $J = 1$  model. Can this analogy be pressed further? A moment's reflection will confirm that the two systems are equivalent to each other under a checkerboard symmetry operation. If you take an infinite  $J = 1$  system in some state and flip all the spins that lie on the black squares of an infinite checkerboard, and set  $J = -1$  (figure 31.8), then the energy is unchanged. (The magnetization changes, of course.) So all thermodynamic properties of the two systems are expected to be identical in the case of zero applied field.

But there is a subtlety lurking here. Have you spotted it? We are simulating finite grids with periodic boundary conditions. If the size of the grid in any direction is *odd*, then the checkerboard operation is no longer a symmetry operation relating  $J = +1$  to  $J = -1$ , because the checkerboard doesn't match up at the boundaries. This means that for systems of odd size, the ground state of a system with  $J = -1$  will have degeneracy greater than 2, and the energy of those ground states will not be as low as  $-2$  per spin. So we expect qualitative differences between the cases  $J = \pm 1$  in odd-sized systems. These differences are expected to be most prominent for small systems. The frustrations are introduced by the boundaries, and the length of the boundary grows as the square root of the system size, so the fractional influence of this boundary-related frustration on the energy and entropy of the system will decrease as  $1/\sqrt{N}$ . Figure 31.9 compares the energies of the ferromagnetic and antiferromagnetic models with  $N = 25$ . Here, the difference is striking.



### Triangular Ising model

We can repeat these computations for a triangular Ising model. Do we expect the triangular Ising model with  $J = \pm 1$  to show different physical properties from the rectangular Ising model? Presumably the  $J = 1$  model will have broadly similar properties to its rectangular counterpart. But the case  $J = -1$  is radically different from what's gone before. Think about it: *there is no unfrustrated ground state*; in any state, there *must* be frustrations – pairs of neighbours who have the same sign as each other. Unlike the case of the rectangular model with odd size, the frustrations are not introduced by the periodic boundary conditions. *Every set of three mutually neighbouring spins must be in a state of frustration*, as shown in figure 31.10. (Solid lines show ‘happy’ couplings which contribute  $-|J|$  to the energy; dashed lines show ‘unhappy’ couplings which contribute  $|J|$ .) Thus we certainly expect different behaviour at low temperatures. In fact we might expect this system to have a non-zero entropy at absolute zero. (‘Triangular model violates third law of thermodynamics!’)

Let's look at some results. Sample states are shown in figure 31.12, and figure 31.11 shows the energy, fluctuations, and heat capacity for  $N = 4096$ .

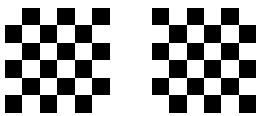


Figure 31.7. The two ground states of a rectangular Ising model with  $J = -1$ .

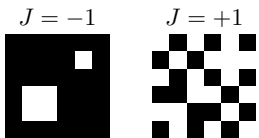


Figure 31.8. Two states of rectangular Ising models with  $J = \pm 1$  that have identical energy.

Figure 31.9. Monte Carlo simulations of rectangular Ising models with  $J = \pm 1$  and  $N = 25$ . Mean energy and fluctuations in energy as a function of temperature.

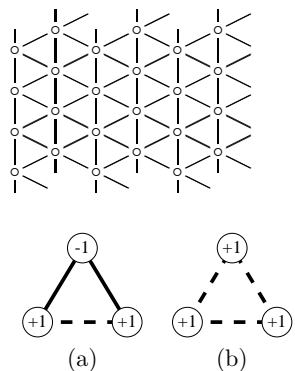


Figure 31.10. In an antiferromagnetic triangular Ising model, any three neighbouring spins are frustrated. Of the eight possible configurations of three spins, six have energy  $-|J|$  (a), and two have energy  $3|J|$  (b).

### 31.2: Direct computation of partition function of Ising models

407

Note how different the results for  $J = \pm 1$  are. There is no peak at all in the standard deviation of the energy in the case  $J = -1$ . This indicates that the antiferromagnetic system does not have a phase transition to a state with long-range order.

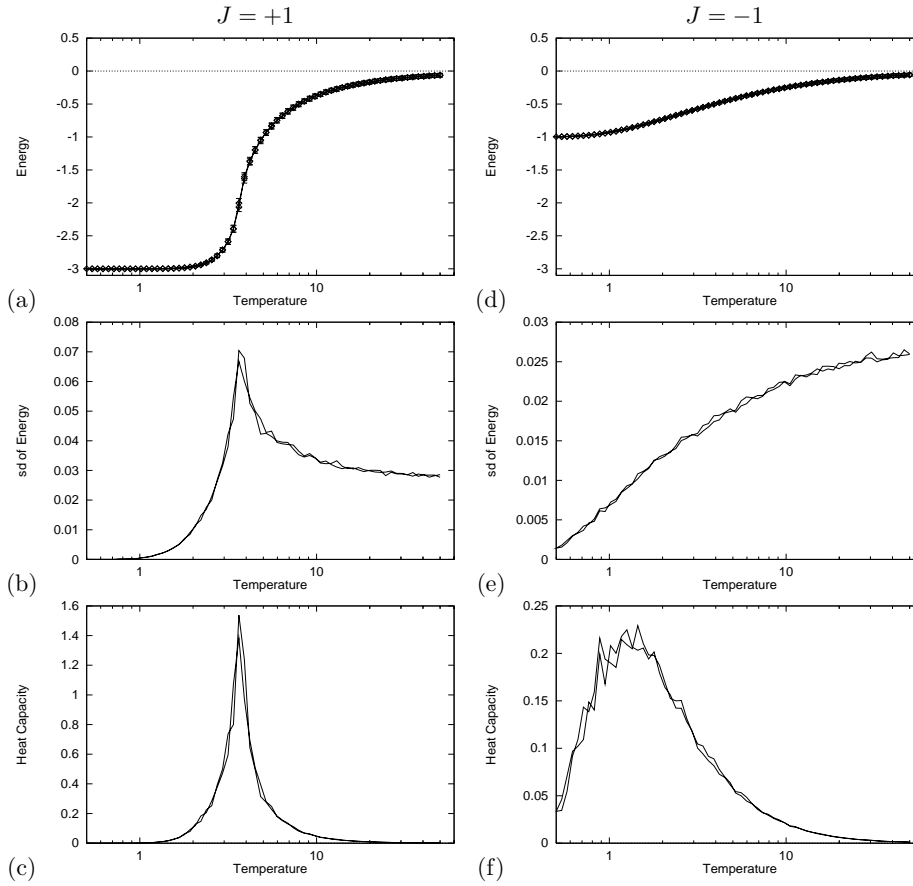


Figure 31.11. Monte Carlo simulations of triangular Ising models with  $J = \pm 1$  and  $N = 4096$ . (a–c)  $J = 1$ . (d–f)  $J = -1$ . (a, d) Mean energy and fluctuations in energy as a function of temperature. (b, e) Fluctuations in energy (standard deviation). (c, f) Heat capacity.

### ► 31.2 Direct computation of partition function of Ising models

We now examine a completely different approach to Ising models. The *transfer matrix method* is an exact and abstract approach that obtains physical properties of the model from the partition function

$$Z(\beta, \mathbf{J}, \mathbf{b}) \equiv \sum_{\mathbf{x}} \exp[-\beta E(\mathbf{x}; \mathbf{J}, \mathbf{b})], \quad (31.25)$$

where the summation is over all states  $\mathbf{x}$ , and the inverse temperature is  $\beta = 1/T$ . [As usual, Let  $k_B = 1$ .] The free energy is given by  $F = -\frac{1}{\beta} \ln Z$ . The number of states is  $2^N$ , so direct computation of the partition function is not possible for large  $N$ . To avoid enumerating all global states explicitly, we can use a trick similar to the sum-product algorithm discussed in Chapter 25. We concentrate on models that have the form of a long thin strip of width  $W$  with periodic boundary conditions in both directions, and we iterate along the length of our model, working out a set of *partial partition functions* at one location  $l$  in terms of partial partition functions at the previous location  $l - 1$ . Each iteration involves a summation over all the states at the boundary. This operation is exponential in the width of the strip,  $W$ . The final clever trick



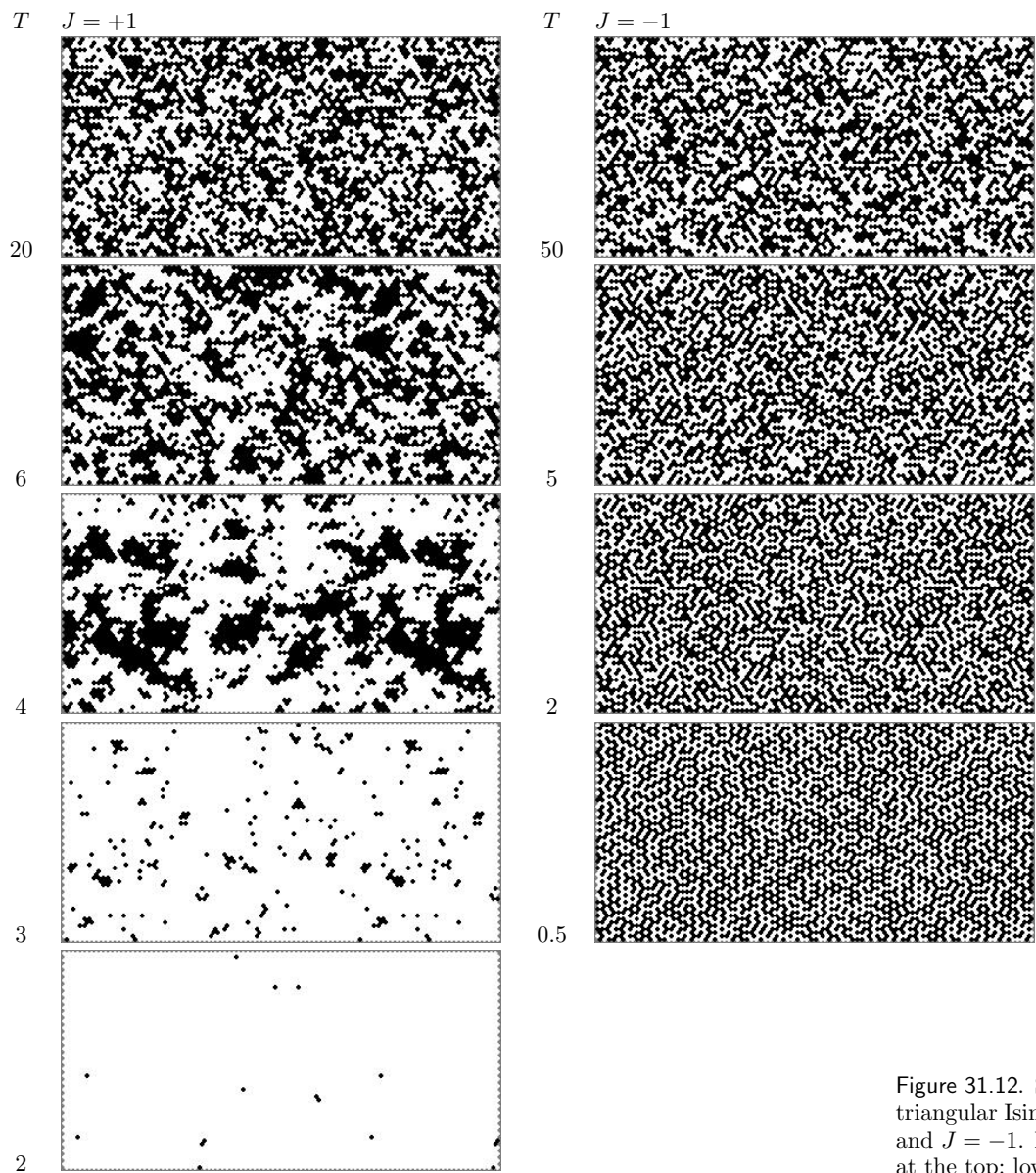


Figure 31.12. Sample states of triangular Ising models with  $J = 1$  and  $J = -1$ . High temperatures at the top; low at the bottom.

### 31.2: Direct computation of partition function of Ising models

409

is to note that if the system is translation-invariant along its length then we need to do only *one* iteration in order to find the properties of a system of *any* length.

The computational task becomes the evaluation of an  $S \times S$  matrix, where  $S$  is the number of microstates that need to be considered at the boundary, and the computation of its eigenvalues. The eigenvalue of largest magnitude gives the partition function for an infinite-length thin strip.

Here is a more detailed explanation. Label the states of the  $C$  columns of the thin strip  $s_1, s_2, \dots, s_C$ , with each  $s$  an integer from 0 to  $2^W - 1$ . The  $r$ th bit of  $s_c$  indicates whether the spin in row  $r$ , column  $c$  is up or down. The partition function is

$$Z = \sum_{\mathbf{x}} \exp(-\beta E(\mathbf{x})) \quad (31.26)$$

$$= \sum_{s_1} \sum_{s_2} \cdots \sum_{s_C} \exp\left(-\beta \sum_{c=1}^C \mathcal{E}(s_c, s_{c+1})\right), \quad (31.27)$$

where  $\mathcal{E}(s_c, s_{c+1})$  is an appropriately defined energy, and, if we want periodic boundary conditions,  $s_{C+1}$  is defined to be  $s_1$ . One definition for  $\mathcal{E}$  is:

$$\mathcal{E}(s_c, s_{c+1}) = \sum_{\substack{(m,n) \in \mathcal{N}: \\ m \in c, n \in c+1}} J x_m x_n + \frac{1}{4} \sum_{\substack{(m,n) \in \mathcal{N}: \\ m \in c, n \in c}} J x_m x_n + \frac{1}{4} \sum_{\substack{(m,n) \in \mathcal{N}: \\ m \in c+1, n \in c+1}} J x_m x_n. \quad (31.28)$$

This definition of the energy has the nice property that (for the rectangular Ising model) it defines a matrix that is symmetric in its two indices  $s_c, s_{c+1}$ . The factors of  $1/4$  are needed because vertical links are counted four times. Let us define

$$M_{ss'} = \exp(-\beta \mathcal{E}(s, s')). \quad (31.29)$$

Then continuing from equation (31.27),

$$Z = \sum_{s_1} \sum_{s_2} \cdots \sum_{s_C} \left[ \prod_{c=1}^C M_{s_c, s_{c+1}} \right] \quad (31.30)$$

$$= \text{Trace} [\mathbf{M}^C] \quad (31.31)$$

$$= \sum_a \mu_a^C, \quad (31.32)$$

where  $\{\mu_a\}_{a=1}^{2^W}$  are the eigenvalues of  $\mathbf{M}$ . As the length of the strip  $C$  increases,  $Z$  becomes dominated by the largest eigenvalue  $\mu_{\max}$ :

$$Z \rightarrow \mu_{\max}^C. \quad (31.33)$$

So the free energy per spin in the limit of an infinite thin strip is given by:

$$f = -kT \ln Z / (WC) = -kTC \ln \mu_{\max} / (WC) = -kT \ln \mu_{\max} / W. \quad (31.34)$$

It's really neat that *all* the thermodynamic properties of a long thin strip can be obtained from just the largest eigenvalue of this matrix  $\mathbf{M}$ !

#### Computations

I computed the partition functions of *long-thin-strip* Ising models with the geometries shown in figure 31.14.

As in the last section, I set the applied field  $H$  to zero and considered the two cases  $J = \pm 1$  which are a ferromagnet and antiferromagnet respectively. I computed the free energy per spin,  $f(\beta, J, H) = F/N$  for widths from  $W = 2$  to 8 as a function of  $\beta$  for  $H = 0$ .

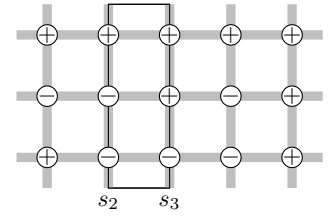


Figure 31.13. Illustration to help explain the definition (31.28).  $\mathcal{E}(s_2, s_3)$  counts all the contributions to the energy in the rectangle. The total energy is given by stepping the rectangle along. Each horizontal bond inside the rectangle is counted once; each vertical bond is half-inside the rectangle (and will be half-inside an adjacent rectangle) so half its energy is included in  $\mathcal{E}(s_2, s_3)$ ; the factor of  $1/4$  appears in the second term because  $m$  and  $n$  both run over all nodes in column  $c$ , so each bond is visited twice.

For the state shown here,  $s_2 = (100)_2$ ,  $s_3 = (110)_2$ , the horizontal bonds contribute  $+J$  to  $\mathcal{E}(s_2, s_3)$ , and the vertical bonds contribute  $-J/2$  on the left and  $-J/2$  on the right, assuming periodic boundary conditions between top and bottom. So  $\mathcal{E}(s_2, s_3) = 0$ .

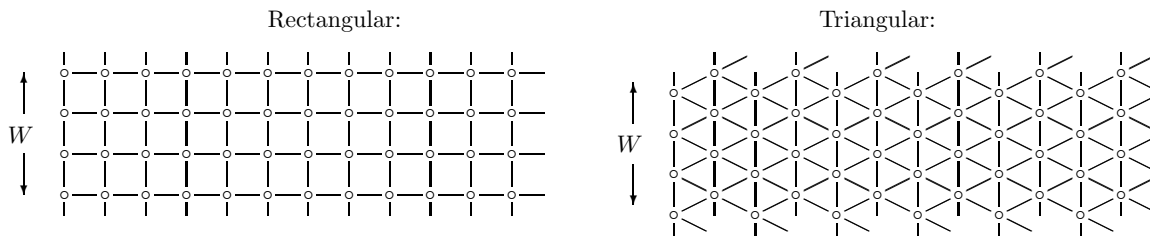


Figure 31.14. Two long-thin-strip Ising models. A line between two spins indicates that they are neighbours. The strips have width  $W$  and infinite length.

### Computational ideas:

Only the largest eigenvalue is needed. There are several ways of getting this quantity, for example, iterative multiplication of the matrix by an initial vector. Because the matrix is all positive we know that the principal eigenvector is all positive too (Frobenius–Perron theorem), so a reasonable initial vector is  $(1, 1, \dots, 1)$ . This iterative procedure may be faster than explicit computation of all eigenvalues. I computed them all anyway, which has the advantage that we can find the free energy of finite length strips – using equation (31.32) – as well as infinite ones.

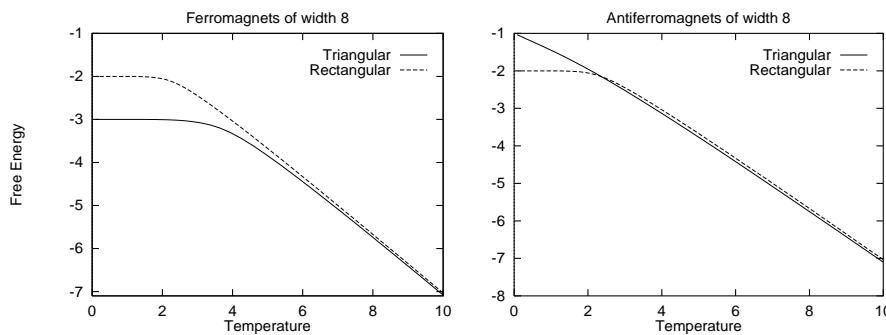


Figure 31.15. Free energy per spin of long-thin-strip Ising models. Note the non-zero gradient at  $T = 0$  in the case of the triangular antiferromagnet.

### Comments on graphs:

For large temperatures all Ising models should show the same behaviour: the free energy is entropy-dominated, and the entropy per spin is  $\ln(2)$ . The mean energy per spin goes to zero. The free energy per spin should tend to  $-\ln(2)/\beta$ . The free energies are shown in figure 31.15.

One of the interesting properties we can obtain from the free energy is the degeneracy of the ground state. As the temperature goes to zero, the Boltzmann distribution becomes concentrated in the ground state. If the ground state is degenerate (i.e., there are multiple ground states with identical

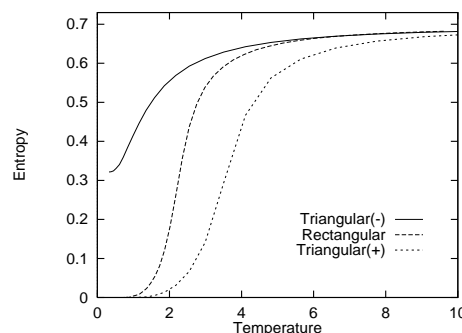


Figure 31.16. Entropies (in nats) of width 8 Ising systems as a function of temperature, obtained by differentiating the free energy curves in figure 31.15. The rectangular ferromagnet and antiferromagnet have identical thermal properties. For the triangular systems, the upper curve (–) denotes the antiferromagnet and the lower curve (+) the ferromagnet.

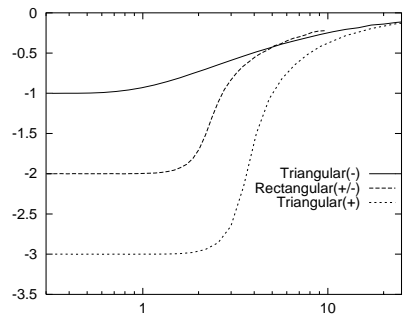


Figure 31.17. Mean energy versus temperature of long thin strip Ising models with width 8. Compare with figure 31.3.

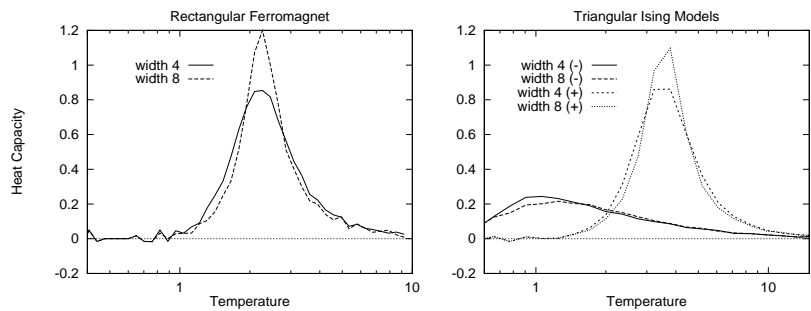


Figure 31.18. Heat capacities of (a) rectangular model; (b) triangular models with different widths, (+) and (-) denoting ferromagnet and antiferromagnet. Compare with figure 31.11.

energy) then the entropy as  $T \rightarrow 0$  is non-zero. We can find the entropy from the free energy using  $S = -\partial F/\partial T$ .

The entropy of the triangular antiferromagnet at absolute zero appears to be about 0.3, that is, about half its high temperature value (figure 31.16). The mean energy as a function of temperature is plotted in figure 31.17. It is evaluated using the identity  $\langle E \rangle = -\partial \ln Z/\partial \beta$ .

Figure 31.18 shows the estimated heat capacity (taking raw derivatives of the mean energy) as a function of temperature for the triangular models with widths 4 and 8. Figure 31.19 shows the fluctuations in energy as a function of temperature. All of these figures should show smooth graphs; the roughness of the curves is due to inaccurate numerics. The nature of any phase transition is not obvious, but the graphs seem compatible with the assertion that the ferromagnet shows, and the antiferromagnet does not show a phase transition.

The pictures of the free energy in figure 31.15 give some insight into how we could predict the transition temperature. We can see how the two phases of the ferromagnetic systems each have simple free energies: a straight sloping line through  $F = 0$ ,  $T = 0$  for the high temperature phase, and a horizontal line for the low temperature phase. (The slope of each line shows what the entropy per spin of that phase is.) The phase transition occurs roughly at the intersection of these lines. So we predict the transition temperature to be linearly related to the ground state energy.

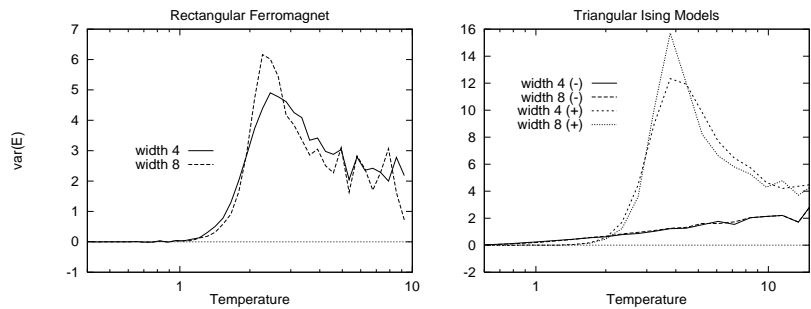


Figure 31.19. Energy variances, per spin, of (a) rectangular model; (b) triangular models with different widths, (+) and (-) denoting ferromagnet and antiferromagnet. Compare with figure 31.11.

### *Comparison with the Monte Carlo results*

The agreement between the results of the two experiments seems very good. The two systems simulated (the long thin strip and the periodic square) are not quite identical. One could a more accurate comparison by finding all eigenvalues for the strip of width  $W$  and computing  $\sum \lambda^W$  to get the partition function of a  $W \times W$  patch.

## ► 31.3 Exercises

- ▷ Exercise 31.2.<sup>[4]</sup> What would be the best way to extract the entropy from the Monte Carlo simulations? What would be the best way to obtain the entropy and the heat capacity from the partition function computation?



Exercise 31.3.<sup>[3]</sup> An Ising model may be generalized to have a coupling  $J_{mn}$  between any spins  $m$  and  $n$ , and the value of  $J_{mn}$  could be different for each  $m$  and  $n$ . In the special case where all the couplings are positive we know that the system has two ground states, the all-up and all-down states. For a more general setting of  $J_{mn}$  it is conceivable that there could be *many* ground states.

Imagine that it is required to make a spin system whose local minima are a given list of states  $\mathbf{x}_{(1)}, \mathbf{x}_{(2)}, \dots, \mathbf{x}_{(S)}$ . Can you think of a way of setting  $\mathbf{J}$  such that the chosen states are low energy states? You are allowed to adjust all the  $\{J_{mn}\}$  to whatever values you wish.